Original Research

Responses of Performance and Microbial Community to Long-Term Graphene Oxide Exposure in a Sequencing Batch Reactor

Jinghou Wang[1#], Liqiu Zhang[2,3#], Shaoqing Zhang[3], Shugeng Li[1,2*], Hainan Yao[3]

[1]School of Environmental Science and Engineering, Guangzhou University, Guangzhou 510006, PR China
[2]Key Laboratory for Water Quality and Conservation of the Pearl River Delta, Ministry of Education,
Guangzhou University, Guangzhou 510006, PR China
[3] School of Civil Engineering, Guangzhou University, Guangzhou 510006, PR China

Abstract

The widespread use of graphene oxide (GO) raises environmental concerns. Municipal wastewater treatment systems are potential receptors of GO containing streams, yet the influences of chronic toxicity of GO on these systems are poorly understood. In the present study, the responses of nutrient removal performance and microbial community to long-term GO exposure were investigated. The results showed that reduction in performance of COD, ammonia and phosphate removals was observed during the whole experiment. The highest effluent COD contents 56.07 mg/L occurred when influent GO concentration was 30 mg/L. Low concentration of GO (1-10 mg/L) had a greater impact on ammonia and phosphate removal performance, the highest effluent concentration of ammonia and phosphate was 9.51 mg/L and 2.72 mg/L. However, there was a certain recovery trend of removal efficiency in each concentration gradient. The results of 16S rRNA gene sequencing showed that long-term GO exposure significantly altered the composition and structure of activated sludge microbial communities. Specifically, both bacterial richness and evenness indexes decreased as the GO concentration increased. Significant shift of bacterial community structures was observed after GO addition and then recover slightly at recovery stage without GO addition. Moreover, functional bacteria, such as *Dechloromonas*, *Nitrosomonas*, *Nitrospira*, *Defluviicoccus,* and *Chryseobacterium* were significantly shifted, which may be associated with altered nutrient removal performances and EPS production. And protein content in EPS varied between 103.54 mg/L and 206.84 mg/L. The findings in this study provide new insights into our understanding of the potential effects of long-term GO exposure on wastewater treatment systems.

Keywords: graphene oxide, chronic toxicity, activated sludge, functional bacteria, community structure

#These authors contributed equally to this study.
*e-mail: lishugeng@gzhu.edu.cn

Introduction

Due to the unique physical and chemical properties, graphene oxide (GO) have been widely used in multifunctional sensor materials [1, 2], drug carrier [3, 4], adsorbent material [5-7]. The discharge GO during their production and use inevitably lead to the wastewater with GO entering the sewage treatment process. Moreover, GO was widely used as adsorbent in wastewater treatment systems for removal of heavy metal [8, 9], organic dye [10] and refractory organic matters [11]. However, GO has biological toxicity [12] and antibacterial properties [13]. Reactor performance and microbial communities of sewage treatment systems could be influenced because of the existing GO. Therefore, the impact of GO on performances reactor of sewage treatment systems should be a comprehensively evaluated.

The cytotoxicity of GO has been extensively studied in culture system for pure cells. For example, the toxicity of GO has been demonstrated to be related to the particle size, oxygen content, exposure environment of red blood cells [14]. In addition, the decreased oxidation degree of GO led to a higher degree of cytotoxicity [15, 16]. On the contrary, a study indicated that one kind graphene oxide polymer had no conspicuous cytotoxicity to murine macrophages [17]. However, the findings obtained in the studies employed culture systems cannot be generalized to complex microbial communities such as activated sludge systems. Moreover, when the concentration of GO achieved at a low range (50-100 mg/L), GO could play a facilitating role in nitrogen removal system [18].

At present, the cytotoxicity of GO has been widely studied in activated sludge systems [13], soil microbial communities [19]. Akhavan et al. [20] that the graphene oxide nanowalls have toxic to Gram-negative Escherichia coli bacteria. Nguyen et al. [21] investigated the cytotoxicity of 1 and 5 mg/L of GO during 10 days in activated sludge, the results suggested that impact of GO in nutrient removal and transformations in microbial communities was significant. Liu et al. [22] mentioned, 0.06 g/L GO might conquer bioactivity of phosphorus-accumulating organisms in activated sludge system, the text sustained a few hours. However, not all research results were negative, Guo [23] recommended that GO could be combined with sludge perfectly and promoted the bioactivities of some functional bacteria. Ahmed [24] demonstrated that in the activated the presence of GO influenced metabolic activity and viability of the bacterial, in concentration between 5 and 300 mg GO/L. Overall, the previous study indicated that short-term GO exposure could have different effects on

microorganisms, i.e., low concentration of GO might have positive impact on nitrogen removal, while high concentration of GO would inhibit the activity of microorganisms. However, GO could adsorb on the sludge [25] and the SRT is longer about 10-25 days [26]. Therefore, GO might accumulate in the sludge have chronic effects on biological treatment systems. Long-term GO exposure is rarely reported.Therefore, the aim of this study is to investigate the impact of long-term GO exposure on rector performance and microbial structure and abundance of sewage treatment system. To achieve these goals, SBR reactors was used. The concentration of GO was set as 1, 2, 5, 10, 15, 30, 60, 80 mg/L and Without GO, and each concentration lasted 10 cycles. The purpose was to determine the relationship between the accumulation of graphene oxide in activated sludge and the change of effluent, and the changes in microbial diversity structure and abundance.

Materials and Methods

Preparation and Characteristics of GO

The purchased GO aqueous solution purchased from Nanjing XFNANO Materials Tech Co., Ltd has a concentration of 2000 mg/L. The GO has a single layer ratio of about 99%, a thickness of 0.8 to 1.2 nm, a purity of about 99%, and a sheet diameter of less than 500 nm. The GO solution was stored in dark. The different dosage of GO solution was added to prepare different concentration influent in the experiment (Table 1). GO in the supernatant were quantified using a UV-Visible spectrophotometer (UV-2550, Shimadzu, Japan) with minimum detection limit of 1 mg/L. To avoid interference from the background of the biomass supernatant, a wavelength of 300 nm was used for GO quantification [27].

Reactor Setup

Two identical SBR reactors were set up, one for the test group and the other for the control group. Both reactors were seeded with activated sludge obtained from a secondary clarifier of a Lek Kok Sewage Treatment Plant (Guangzhou, China). The working volume was 4 L with a cylindrical part height of 310 cm, lower cone height of 90 cm and an inner diameter of 15 cm. The SBR was worked at 26±2ºC with two cycles each day. Each cycle was consisted of 120 min anaerobic stage, 240 min aerobic stage, 30 min settle time, 10 min draw and about 5.3 h idle. Drainage ratio was 50%. The hydraulic retention time (HRT)

Table 1. GO concentrations in different cycles.

Cycle	1-10	11-20	21-30	31-40	41-50	51-60	61-70	71-80	81-90
Concentration (mg/L)	1	2	5	10	15	30	60	80	Without GO

Table 2. Composition of synthetic wastewater.

Ingredients	Concentration (mg/L)	Ingredients	Concentration (mg/L)
NH_4^+-N	23.99~30.95	COD	288.36~301.71
NO_3^--N	0.92~1.73	PO_4^{3-}	2.42~3.42
NO_2^--N	0~0.087		

Note: pH was 7.3~7.6.

was set at 6.5 h and the sludge retention time (SRT) was set at 20±2 days, MLSS was maintained at 4500±450 mg/L with 200 mL mixed liquor discharging from the reactor per day. The reactors were fed with synthetic wastewater (Table 2) in the first 1 min of the anaerobic stage every 12 h. COD was supplemented with glucose in synthetic wastewater. The reactor pH was adjusted to 7.0 by adding $NaHCO_3$ and 3M HCl. In the aerobic phase, the aerated air flow rate was 40 L/h to maintain simultaneous phosphate and nitrogen removal. Both reactors were pre-cultivated for 10 days to achieve stable activity. Afterward, they were operated for 90 cycles, along with GO added to test reactor (Table 1) and without GO adding for control reactor.

Chemical Parameter Analysis

For each cycle, the effluent of two reactors was analyzed for the following parameters: ammonia (NH_4^+-N), total nitrogen (TN), phosphate (PO_4^{3-}), and chemical oxygen demand (COD). After collected, influent and effluent were filtered through 0.1~0.3 μm qualitative filter paper (Sangon Biotech, Shanghai. Co., Ltd.). NH_4^+-N,PO_4^{3-} and nitrite nitrogen were analyzed according to the national standard methods [28] using UV-2550 uv-visible spectrophotometer (SHIMADZU). All chemical indicators were in the unit of mg/L.

Extracellular Polymeric Substances (EPS) Analysis

EPS was excecated using modified heat extraction [29, 30]. All samples were taken from the end of the anaerobic phase at the end of each concentration gradient. At the end of a cycle, 10 mL of the mixed liquor in the reactor was taken with a 10 mL syringe and transferred to a 15 mL centrifuge tube. After the precipitation for 10 min, the supernatant was decanted, and the sludge was washed three times with 10 mL of phosphate buffered saline (PBS) (30 min once). The volume was adjusted to 10 mL, and the mixture was centrifuged at 4ºC, 4000 rpm for 20 min, and the supernatant was collected (dissolved EPS). The sludge was resuspended in 10 mL of pure water, and 4 mL of a 1 mol/L sodium hydroxide solution was added and stored at 4ºC for 3 hours. Then, the mixture was stirred for 35 minutes at 400 rpm and 80ºC. Finally, high-speed centrifugation (10000×g, 20 min, 4ºC) was used to extract the combined extracellular polymer.

The supernatant was used for EPS chemical composition analysis. Particulates in samples were removed using a 0.45 μm polytetrafluoroethylene (PTFE) membrane prior to EPS chemical composition analysis. EPS included protein (PN) and polysaccharide (PS). With Modified BCA Protein Assay Kit (Sangon Biotech, Shanghai. Co., Ltd.) and phenol-sulphuric acid method, the PN and PS contents were also analyzed by UV–vis spectrophotometry [31].

DNA Extraction and Quantitative Real-Time PCR (q-PCR)

Biomass samples from the test reactor were collected at the end of the anaerobic phase at the end of each concentration gradient. Using filter paper (11 cm, 45 μm) to filter the obtained mixed liquid sludge samples and weighed 0.25 g for DNA extraction. Extraction of DNA using the Power Soil DNA Isolation Kit (Mobio, USA).

The q-PCR was guided by using q-PCR kit (SYBR Green PCR master mix, Sangon Biotech (Shanghai), China) in term of the manufacturer's instructions on StepOne Plus Real-Time PCR System (Applied Biosystems, Thermofisher, USA). We evaluated three functionally genes *amoA* (ammonia monooxygenase), *Nitrospira* and *nirS* (nitrite reductase). The specific primer for amplification of gene *amoA* were CTO189fA/B[b] (GGAGRAAAGCAGGGGATCG), CTO189fC[b] (GGAGGAAAGTAGGGGATCG) and RT1r (CGTCCTCTCAGACCARCTACTG) [32]. The specific primer sets for amplification of *Nitrospira* gene were NSR1113f (CCTGCTTTCAGTTGCTACCG) and NSR1264r (GTTTGCAGCGCTTTGTACCG)[33]. The specific primer for amplification of gene *nirS* were Cd3aF (GTSAACGTSAAGGARACSGG) [34] and R3cdR (GASTTCGGRTGSGTCTTGA) [35]. A 25 μl reaction system was set up for each PCR amplification, including 9.5 μl DEPC treatment water, 1 μl forward primer, 1 μl reverse primer and 12.5 μl SYBR. The amplification program for *amoA* consisted of an initial denaturation step at 95ºC for 4 min, 40 cycles of denaturation at 95ºC for 15 s, annealing at 61ºC for 30 s and followed by extension at 72ºC for 1 min. The amplification program for *Nitrospira* consisted of an initial denaturation step at 95ºC for 5 min, 40 cycles

of denaturation at 95ºC for 15 s, annealing at 60ºC for 30 s and followed by extension at 72ºC for 1 min. The amplification program for *nirS* consisted of an initial denaturation step at 95ºC for 4 min, 40 cycles of denaturation at 98ºC for 10 s, annealing at 60ºC for 30 s and followed by extension at 72ºC for 1 min.

Metagenomic Classification and Sequencing

The changes in the microbial community exposed to nanomaterial different concentrations of GO and recovery phase were analyzed using deep sequencing 16S rRNA to understand the chronic toxicity of different concentrations of GO on microorganisms in the reactor. DNA samples were extracted using the E.Z.N.A.TM Soil DNA Kit (Omega Bio-tek, Inc. USA). Genomic DNA was accurately quantified using the Qubit 3.0 DNA Assay Kit to determine the amount of DNA that should be added to the PCR reaction. The primers (341F Primer: CCCTACACGACG CTCTTCCGATCTG (barcode) CCTACGGGNGGCW GCAG, 805R Primer: GACTGGAGTTCCTT GGCACCCGAGAATTCCAGACTACHV GGGTAT CTAATCC) used in PCR have been fused to the V3-V4 universal primers of the Miseq sequencing

platform. Two rounds of DNA amplification were according to the protocol described in the preparation of the 16S rRNA Metagenomics sequencing library in the Illumina protocol. For PCR products amplified by bacteria and archaea and normal amplified fragments, the PCR product of 400 bp or more was treated with 0.6 times of magnetic beads (Agencourt AMPure XP). The recovered DNA was accurately quantified using the Qubit 3.0 DNA Assay Kit to facilitate sequencing in an equal amount of 1:1. When mixed in equal amounts, the amount of DNA per sample was 10 ng, and the final sequencing concentration was 20 pmol. The DNA-amplified samples were sequenced using an Illumina MiSeq sequencer.

Results and Discussions

Impact of GO on COD, NH_4^+-N, TN and PO_4^{3-} Removal

In biological treatment, COD was not only a means to determine the quality of biological processes, but also to reflect the activity of activated sludge [36]. Table S1 shows GO had a great impact on COD, TN and
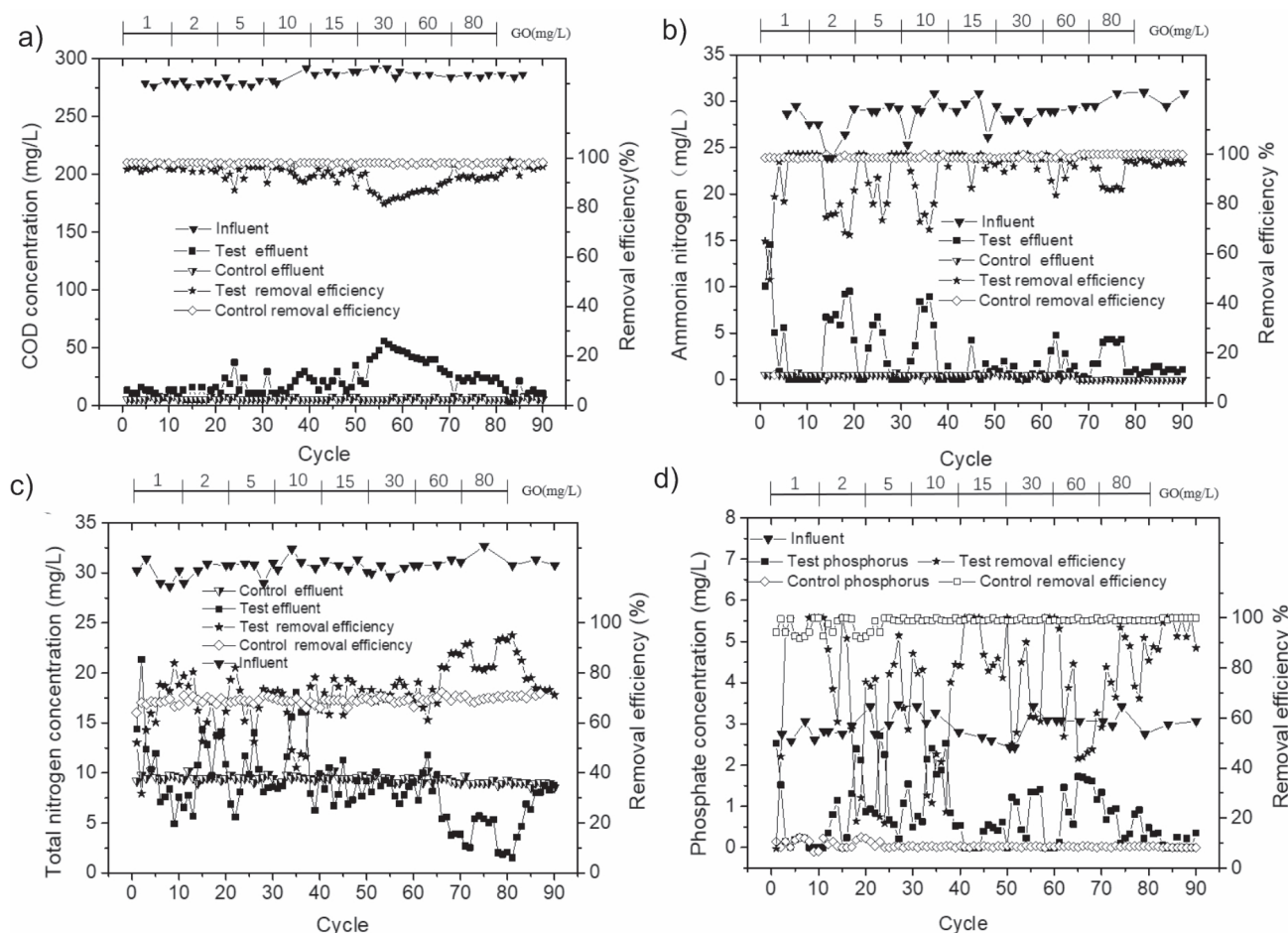

Fig. 1. COD a), NH_4^+ -N(b), TN c) and PO_4^{3-} d) in the influent and effluent of controls and reactors treated with different concentrations of GO.

P concentration (*P*<0.01). Fig. 1a) shows COD changes in the test group and the control. As seen in Fig. 1a), the COD of the control group was stable at around 5 mg/L from the end of set-up and removal efficiency of COD was up to 98%. Almost all the effluent COD of the experimental group was higher than the control group, apart from one data point at recovery phase, and it was 2.67 mg/L. When the concentration of GO was 5 mg/L, COD in the effluent increased and then decreased after five cycles, and the peak value was 37.38 mg/L (the GO accumulate in activity sludge was 24 mg/L), removal efficiency dropped to 87%. From the 35th to 39th cycle, the effluent COD of the experimental group gradually increased, indicating that microbial activity in the activated sludge were gradually inhibited. As seen in Table S2, changes of GO could be reflected. During cycle 40-52, the average COD effluent decrease to 20.74 mg/L, but obviously higher than control, removal efficiency was about 92%. Then COD increase again, until cycle 56, the higher COD effluent was up to 56.07 mg/L, and the GO accumulation in activated sludge was 135.67 mg/L. After that, COD effluent decrease steadily until cycle 70. Then even GO concentration increased to 80 mg/L, COD kept stable at 20 mg/L. When GO was no longer added, the COD of the experimental group in the effluent could gradually decreased and kept stable around 10 mg/L.

The impacts on COD removals in activated sludge were previously reported with carbon-based nanomaterials in long- or short-term assays [21, 24, 37, 38]. For instance, acute toxicity studies with MWCNT and G agreed with each other that low concentrations (1 mg/L) of these nanomaterials for short time did not impact COD removal [37, 38]. Chronic study with continuously fed with GO or G showed that COD removal reduced significantly after nanomaterial accumulation in the activated sludge reached certain contents [39], which was consistent with our results. The initial low concentration of GO had little effect on COD removal efficiency. With the accumulation of GO in sludge, the influence gradually strengthened. However, due to the adaption of microorganisms to GO, the influence decreased even when the influent GO concentration was higher than before (GO 80 mg/L)Nitrogen and phosphorus are the main factors that cause eutrophication of water bodies, so they are also two important nutrients that should be removed during biological wastewater treatment [40]. The operation mode of the reactor in this experiment was to provide the anaerobic and aerobic conditions of the activated sludge, so that the activated sludge absorbs excess phosphorus after releasing phosphorus. After anaerobic process, the aeration process helps to remove these pollutants in the form of ammonia (NH_3 -N) and phosphate (PO_4^{3-}). The effluent ammonia of control reactor was almost zero and removal efficiency of ammonia was more than 99%. As to test group reactor, except for the first two cycles, the ammonia removal efficiency for all other cycles exceeded 60% (Fig. 1b).

When the GO concentration was 2, 5, 10, 60, 80 mg/L, for each stage, the ammonia nitrogen in the effluent rose to the peak and then decreases. The peak values were 9.51, 6.73, 8.96, 4.77 and 4.32 mg/L, respectively. Peak decreasing indicated that the ammonia-oxidizing bacteria (AOB) in the activated sludge was adapting to the environment in which the GO existed, as evidenced by the EPS analysis - as the activated sludge adapted to the environment of GO, the activated sludge under high concentration of GO did not produce excessive EPS (Fig. 2).

In order to show more detailed effects of GO on nitrogen removal, TN trends were shown in Fig. 1c). For control reactor, TN in effluent kept at 9.5 mg/L, removal efficiency of which remained at 70%. As for test reactor, when GO addition was 1, 2, 5, and 10 mg/L in influent, TN in effluent increased firstly and then decreased to lower than control. When GO concentration was 15 to 80 mg/L, most effluent TN concentration of test group reactor was lower than control. It is worth point out that lowest TN concentration occurred during GO was 80 mg/L. During recovery stage (cycle 80-90), TN in test group recovered to the control. It could conclude that the negative effects of GO on denitrification was low and high concentration of GO could even promote the denitrification. Only when GO concentration was 10 mg/L, denitrification was inhibited. Possible explanation may be the denitrifying bacteria was not inhibited by GO and GO could even increase the quantity of these microorganism, which was proved in the microbial communities' analysis.

Not only was the nitrogen removal efficiency affected by the low concentration of GO, but the phosphate (PO_4^{3-}) removal effect was also slightly changed. Ahmed F. et al. demonstrated that the significant effect of GO on PAO microbial community was observed at higher concentrations of GO (200-300 mg/L) [24], but missing data of long-term accumulation of low concentration GO for
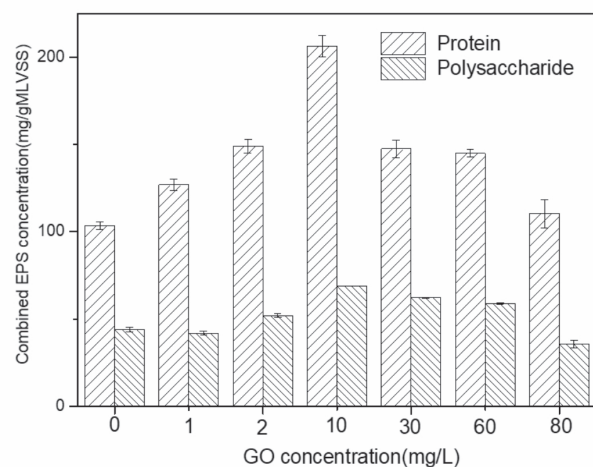

Fig. 2. The concentrations of EPS under the influence of various GO doses.

polyphosphate bacteria in activated sludge. As seen in Fig. 1d), the low concentration of GO had a greater effect on the effluent phosphate. With initially GO adding, phosphate concentration increased fast, but could recover quickly. With the increase of GO, the Phosphate content in the effluent increased again, and it was difficult to return to the level of the control group. Until the GO was 15 mg/L, the Phosphate content in the effluent decreased to the control level. When the GO concentration increases again, the Phosphate content in the effluent still increased, and the maximum concentration was 1.72 mg/L (the influent GO concentration was 60 mg/L), lower than the highest phosphate effluent concentration of 2.72 mg/L (theinfluent GO concentration was 5 mg/L). When the concentration of GO was 80 mg/L, the maximum concentration of Phosphate was 0.911 mg/L, showing that there was still a certain degree of recovery. In the recovery phase of 80-90 cycles (without GO adding), the content of phosphate could be further reduced, and the effluent Phosphate concentration was about 0.3, which indicated that microbial community functionality for phosphate removal had been restored. In the environment of high concentration of GO, PAO had adapted to the new environment, and the phosphate removal capacity had recovered basically. In Hai's study, the authors showed that the microbial population was not able to adapt and recover overtime from the high initial dose (20 mg/L) of nanomaterials [41]. In our study, initial GO concentration was low, and GO concentration was gradually increased, and this allowed the PAO to gradually adapt to the presence of GO and got recovery.

Impact of GO on EPS and SEM Image

As shown in Fig. 2, the change of PS in EPS was not obvious, and the change of PN had a significant increase and then decrease trend. And according to Shah's study [42], we could clearly identify the existence of GO. The description of EPS change below was all about PN. EPS contents increased with GO concentration within 1, 2 and 10 mg/L, and the highest EPS of 206.18 mg/g MLSS occurred at 10 mg/L GO. It is well known that EPS had a function of resisting toxicants as a protective barrier in some toxic environments [43]. Higher EPS contents indicated that microorganisms were under the inhibition of GO. With the increase concentration of GO from 1 to 10 mg/L in the influent, the inhibitory effect was increasing gradually. During the 20 cycles of adding 2, 10 mg/L GO, the ammonia nitrogen concentration had a larger peak compare to the effluent at a higher concentration of GO, indicated that these two concentrations of GO had a greater influence on ammonia removal efficiency during the continuously feeding period. The above result was consistent with the higher concentration of EPS in Fig. 2. This was due to the higher and higher accumulation of GO in activated sludge, which resulted in the inhibition gradually strengthened. COD continued to rise to 29.37 mg/L after 10 mg/L GO was added in the experimental group (Fig. 1a).

From the SEM image (Fig. 3), it was found that bacterial cells in the sludge were broken.in low GO concentration (10 mg/L), which also resulted in the high EPS. As the GO concentration increased to 30 mg/L, the EPS concentration gradually decreased to 147.46 mg/g MLSS. When the GO concentration was 80 mg/L, the EPS concentration decreased to 110.23 mg/g MLSS, which was only a little higher than control group of 103.54 mg/g MLSS. The results meant that although GO centration in the influent increased, the inhibitory effect was attenuated. The possible explanations may be: (1) With the accumulation of GO, some microorganisms adapted to the new situation and reproduced; while some others couldn't survive which lead to the decrease in community richness and diversity (Table 3). As a result, the EPS reduced compared to the initial situation and the inhibition weakened. (2) When the GO concentration was 60 mg/L, microorganisms attached on the GO and no rupture occurred, which was consistent with EPS
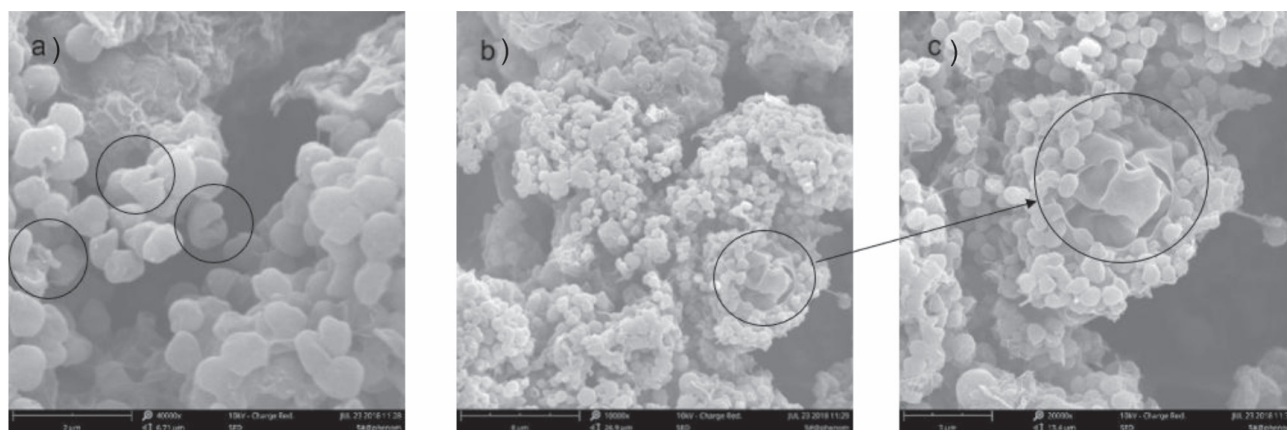

Fig. 3. SEM image of Activated sludge with GO. a) activated sludge with a concentration of 10 mg/L (Bacterial rupture); b), c) activated sludge with a concentration of 60 mg/L (Microbial community attached to GO).

Table 3. Bacterial alpha diversity index statistics.

Sample ID	Seq num	OTU num	ACE index	Chao index	Shannon index	Simpson	Coverage
Control reactor	68798	4771	60396.92	26951.18	5.16	0.03	0.95
10 mg/LGO	51072	3416	47685.87	22229.91	4.42	0.09	0.95
60 mg/LGO	69669	3434	46427.71	25943.37	4.11	0.14	0.96
80 mg/LGO	69948	1560	8167.65	4994.27	2.44	0.33	0.99
Without GO	82935	2067	13328.51	7140.02	3.15	0.24	0.98

decrease. Baek's results [44] showed that bacteria was easy to adsorbed on GO layers. In our study, only when the GO concentration was high enough the GO layer could form and the inhibition could decrease. And as the Table S2 shows that almost all GO was adsorbed into activated sludge.

Considered with the SEM image (Fig. 3a-c), it could be seen that there were signs of bacterial cell destruction in the activated sludge at low concentration of GO. In the image with GO 60 mg/L, the microorganism adhered to the surface of the large piece of graphene oxide sheet, which reduced the damage of the bacteria [45, 46]. There are obvious wrinkles on the GO's surface, maybe it was speculated that high concentration of GO had less inhibitory effect on phosphorus removal [47].

Changes in the Sludge Functional Microbial Communities Exposed to GO

As shown in Table 2, 51072-82935 effective sequences for five activated sludge samples were obtained by 16S rRNA Metagenomics sequencing, and the effective sequence ratio was higher than 95%. The library size of each sample was normalized to 51072 sequences, which was the lowest number of sequences among the five samples. There were total of 15248 OTUs recovered from five activated sludge samples. The coverage values of the five samples were greater than 0.95, which indicated that the sequences covered most the community diversities of these samples. It was obvious that the numbers of OTUs, ACE, Chao, Shannon and Simpson indexes of the five samples were different from each other, suggesting that long-term addition of increased concentration of GO in the influent certainly impacted the microbial communities. Especially, the OTU number decreased from 4771 to 3416 with GO concentration increased from 0 to 10 mg/L, then decreased from 3434 to 1560 with GO concentration increased from 60 to 80 mg/L, demonstrating that increasing GO could weaken the abundance and species richness in this activated sludge systems. Similarly, when GO concentration varied from 0 to 80 mg/L, the values of ACE, Chao, and Shannon also indicated decreased tendencies. However, the OTU number increased from 1560 to 2067 as the GO concentration decreased from 80 mg/L to Without GO, which suggested no longer add GO would strengthen the abundance and species richness. Similarly, the
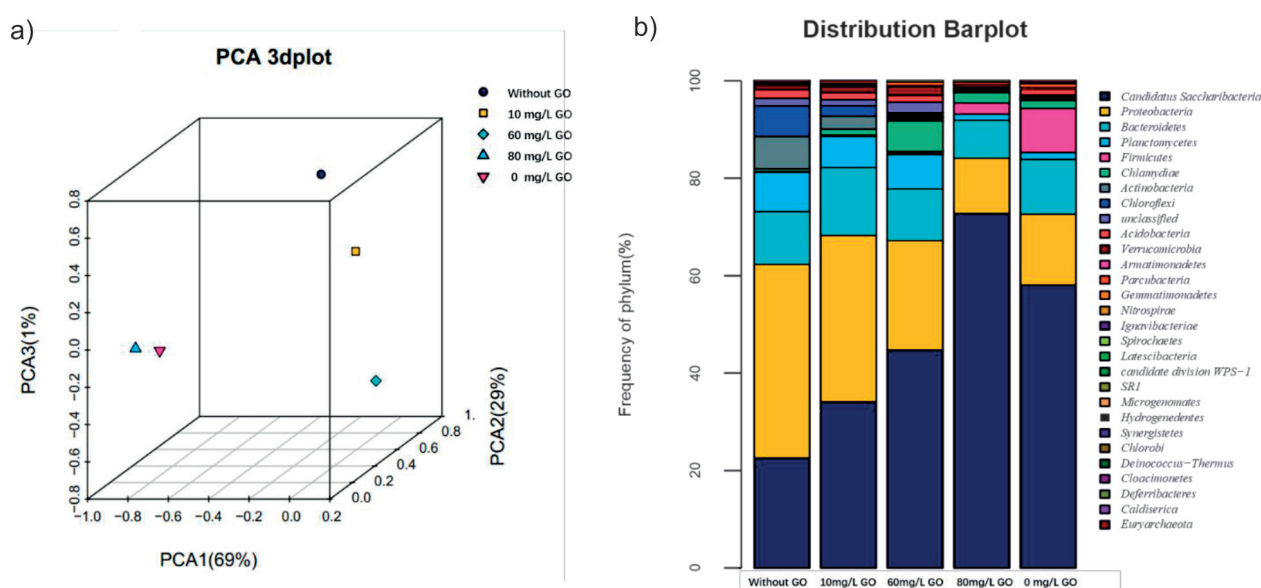

Fig. 4. Community structure of activated sludge system. a) Principal Component Analysis plots of five activated sludge samples. b) Microbial community distribution at the phylum level in each sample.

Table 4. Relative abundances of potential functional groups in test reactor.

Function categories	Genius name	Control reactor (%)	10 mg/L GO (%)	60 mg/L GO (%)	80 mg/L GO (%)	Without GO (%)
GAO	*Defluviicoccus*	9.46	9.57	1.13	0.37	0.54
Bulking bacteria	*Acinetobacter*	0.08	0.03	0	0.08	1
	Chryseobacterium	0	0.14	0	0	0
		0.08	0.17	0	0.08	1
Denitrifier	*Zoogloea*	0.16	0.13	0.22	0.2	0.45
	Thauera	0	0.07	0.12	0.11	0.2
	Pseudomonas	0.02	0	0	0.04	0.34
	Hyphomicrobium	0.15	0.05	0.09	0.04	0.03
	Acidovorax	0.1	0.02	0.06	0.01	0.01
	Flavobacterium	0.02	0.05	0.01	0	0
	Curvibacter	0.01	0.01	0	0	0
	Methylophilus	0	0	0.01	0.01	0
	Paracoccus	0.01	0	0	0	0
		0.47	0.33	0.51	0.41	1.03
NOB	*Nitrospira*	0.17	0.12	0.21	0.07	0.18
		0.17	0.12	0.21	0.07	0.18
AOB	*Nitrosomonas*	0.01	0	0.01	0.02	0.02
	Nitrosospira	0.01	0	0	0	0
		0.02	0	0.01	0.02	0.02

values of ACE, Chao and Shannon also indicated increased tendencies.

PCA (Principal Component Analysis) analysis was completed on the OTU composition of five samples, and the result is shown in Fig. 4a). The contribution rate of principal component 1 (PCA1), principal component 2 (PCA2), and principal component 3 (PCA3) in Fig. 4 were respectively 69%, 29% and 1%. As shown in Fig. 4a), The OTU composition of the activated sludge system at different GO concentrations was quite different, hence the microbial community structure was visibly different. However, the community structure shift was in accordance with the slow changes in flux and biofilm structure at the control reactor. It indicated that the impact of GO to activated sludge system was not permanent.

Five microbial samples at different GO concentrations were analyzed to reveal changes in microbial communities at the phylum level (Fig. 4b). Among the detected 26 known phyla, the relative abundance higher than in each sample were mainly *Proteobacteria* (11.39%~39.8%), *Candidatus Saccharibacteria* (22.55%~72.75%), *Bacteroidetes* (7.75%~13.87%) and *Planctomycetes* (1.42%~8.14%). The relative abundance of *Proteobacteria* in five samples was in order from large to small successively

Control reactor, 10 mg/L GO, 60 mg/L GO, Without GO, 80 mg/L GO. The relative abundance of *Candidatus Saccharibacteria* in activated sludge system when influent GO concentration reach 80 mg/L was the highest, while the relative abundance of *Planctomycetes*, *Chloroflexi* and *Actinobacteria* decreased with the GO concentration increasing.

Candidatus Saccharibacteria and *Proteobacteria* had the highest relative abundance in five samples, they were common dominant phylum in the wastewater treatment process. The experiments of Caroline Kragelund et al. [48] revealed that *Chloroflexi* constituted a specialized group of filamentous bacteria only active under aerobic conditions consuming primarily carbohydrates. The abundance of *Chloroflexi* decreased with GO concentration increased, which resulted in high effluent COD. In addition, the phyla such as *Chlamydiae*, *Planctomycetes*, *Acidobacteria* and *Gemmatimonadetes* were also detected. They all played an important role in the wastewater treatment process though their relative abundance was not high enough.

Table 4 shows the main microbial structure and distribution at genus level in five samples. Among the 324 detected genera, *Defluviicoccus* belonging to glycogen nonpolyphosphate-accumulating organism
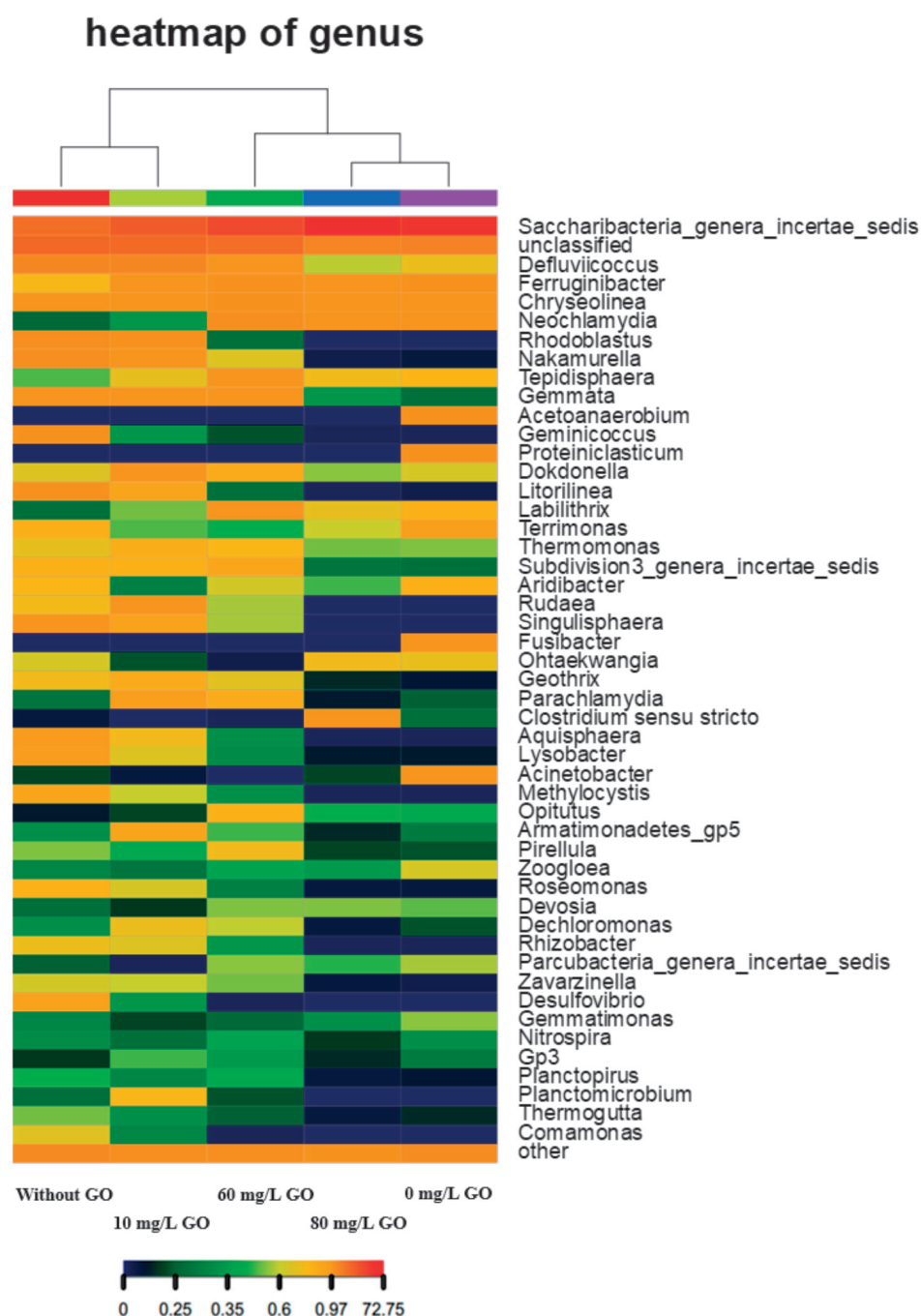
heatmap of genus

Fig. 5. Heatmap of relative abundances of different genera in the reactors with different concentrations of GO. Color scale from Blue (lowest abundance) to Red (highest abundance).

(GAO), which has competition relationship with polyphosphate-accumulating organisms (PAO). Combine Fig. 5 with Fig. 1d), the abundance of *Defluviicoccus* was decreasing constantly, this also indirectly indicated the system environment was more suitable for the growth and reproduction of PAO, which was consistent with the increase in phosphate removal efficiency. *Nitrosomonas* and *Nitrosospira* were two types of AOB detected in this study, the small change in quantity was not enough to explain the impact of GO on it. The abundance of NOB, i.e., *Nitrospira* was

decreased as the concentration of GO increased to 10 mg/L, which was in good agreement with the TN removal efficiency. Some types of Denitrifier such as *Zoogloea*, *Thauera*, *Pseudomonas*, *Hyphomicrobium* and *Acidovorax* were also detected. *Zoogloea* and *Thauera* was less affected. The overall results showed that the GO solution with increasing concentration has a great influence on various functional bacteria in the activated sludge, which changes the community composition of the microorganisms. The q-PCR was conducted to evaluate the abundances of denitrifying
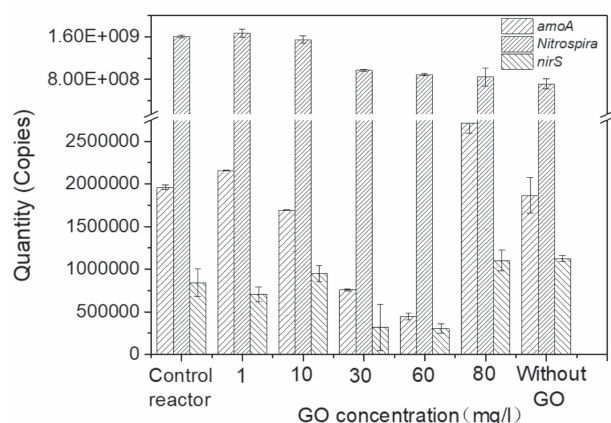
Fig. 6. Quantitative abundances of genes *amoA*, *Nitrospira*, *nirS* at different GO concentrations.

functional genes *nir*S, AOB genes *amo*A and NOB genes *Nitrospira* during the sewage treatment process with GO increased from 0 to 80 mg/L and 10 cycles recovery phase (Fig.6). The three genes showed no obvious changes when GO concentration was 1 mg/L. When GO concentration was increased to 60 mg/L, the abundances of gene *amo*A and *nir*S obviously decreased to 4.43×10^5 copies and 3.02×10^5 copies, respectively, while the decrease tendency of *Nitrospira* presented relatively slight. These results suggested that nitrate reduction ability and ammonia-oxidizing ability were both decreased under high GO concentration, which also indicated that long-term exposure high concentration inhibited the abundances of denitrifying functional genes and AOB genes.

Conclusion

This study investigated the impacts of GO on biological performance and activated sludge microbiota. The conclusions were as follows:

1) In conclusion, GO had a significant impact on COD removal efficiency and the highest effluent COD contents occurred when influent GO concentration was 30 mg/L. Low concentration of GO (1-10 mg/L) had a greater impact on ammonia and phosphate removal performance. And due to the adaption of microorganisms, when the GO concentration is 60 mg/L and 80 mg/L, the phosphate and nitrogen removal efficiency are slightly affected.

2) As GO entered the activated sludge system and combines with it, it adsorbed a large number of microorganisms on the GO surface.

3) As the GO concentration of the influent increased, GO was almost entirely accumulated in the activated sludge, which changed the community structure. Responses of different populations to different GO concentrations were not exactly the same. Kinds of denitrifier were enriched when influent GO was

80 mg/L, which resulted in the lower TN content in the effluent than that of the control reactor. Since GO was not detected in the effluent, the existence of forms and transformation of GO in the sludge will be taken into account in the future study.

Supplementary Data

The following are the supplementary data related to this article: Removal performances of organic and nutrient in the test SBR (Table S1). The quality of GO influent and effluent (Table S2).

Acknowledgement

Conflict of Interest

The authors declare no conflict of interest.

References

1. CHEN Y., PÖTSCHKE P., PIONTECK J., VOIT B., QI H. Smart cellulose/graphene composites fabricated by in situ chemical reduction of graphene oxide for multiple sensing applications. Journal of Materials Chemistry A, **6** (17), 7777, **2018**.

2. HE X., LIU Q., WANG J., CHEN H. Wearable gas/strain sensors based on reduced graphene oxide/linen fabrics [J]. Frontiers of Materials Science, **13** (3), 305, **2019**.

3. CAO M., ZHAO W., WANG L., LI R., GONG H., ZHANG Y., XU H., LU J. Graphene Oxide-Assisted Accumulation and Layer-by-Layer Assembly of Antibacterial Peptide for Sustained Release Applications. ACS Applied Materials & Interfaces, **10** (29), acsami.8b07417-, **2018**.

4. KAZEMPOUR M., NAMAZI H., AKBARZADEH A., KABIRI R., Synthesis and characterization of PEG-functionalized graphene oxide as an effective pH- sensitive drug carrier [J]. Artificial Cells, Nanomedicine, and Biotechnology, **47** (1), 90, **2019**.

5. FAN L., LUO C. SUN M., QIU H., LI X. Synthesis of magnetic β-cyclodextrin-chitosan/graphene oxide as nanoadsorbent and its application in dye adsorption and removal. Colloids & Surfaces B Biointerfaces, **103** (6), 601, **2013**.

6. FAKIR A.A.E., ANFAR Z., BENAFQIR M., JADA A., ALEM N.E. Polyaniline coated hematite sand supported on graphene oxide (HS@PANI-GO) as a new magnetic material for advanced catalytic oxidation based on sulfate radicals: Optimization using response surface methodology [J]. Journal of Chemical Technology & Biotechnology, **94** (8), 2609, **2019**.

7. ZHU H., XU X., ZHONG X. Adsorption of Co(II) on Graphene Oxides from Aqueous Solution[J]. Polish Journal of Environmental Studies, **25** (6), 2675, **2016**.

8. SHERLALA A.I.A., RAMAN A.A.A., BELLO M.M., ASGHAR A. A review of the applications of organo-functionalized magnetic graphene oxide nanocomposites for heavy metal adsorption[J]. Chemosphere, **193**, 1004, **2017**.

9. LIU C.,WU T., HSU P.C., XIE J., ZHAO J., LIU K., SUN J., XU J., TANG J., YE Z. Direct/Alternating Current Electrochemical Method for Removing and Recovering Heavy Metal from Water Using Graphene Oxide Electrode [J]. ACS Nano, **13** (6), 6431, **2019**.

10. TAO X., WANG X., LI Z., ZHOU S. Ultralow temperature synthesis and improved adsorption performance of graphene oxide nanosheets[J]. Applied Surface Science, **324**, 363, **2015**.

11. XU L., MA R., SUN C., SUN D. Enterococcus faecalis Bioflocculant Enhances Recovery of Graphene Oxide from Water[J]. Polish Journal of Environmental Studies, **27** (6), 2811, **2018**.

12. WENDI Z., CHI W., LI Z., LU Z., LI Y., JUN-JIE Y., YU-TING Z., XINGFA G., YING F., GUANGJUN N. Unraveling stress-induced toxicity properties of graphene oxide and the underlying mechanism[J]. Advanced Materials, **24** (39), 5391, **2012**.

13. SEABRA A.B., PAULA A.J., RENATA D.L., ALVES O.L., NELSON D. Nanotoxicity of graphene and graphene oxide[J]. Chemical Research in Toxicology, **27** (2), 159, **2014**.

14. LIAO K.H., LIN Y.S., MACOSKO C.W., HAYNES C.L. Cytotoxicity of Graphene Oxide and Graphene in Human Erythrocytes and Skin Fibroblasts[J]. Acs Appl Mater Interfaces, **3** (7), 2607, **2011**.

15. ZHANG W., YAN L., LI M., ZHAO R., YANG X., JI T., GU Z., YIN J., GAO X., NIE G. Deciphering the underlying mechanisms of oxidation-state dependent cytotoxicity of graphene oxide on mammalian cells. Toxicology Letters, **237** (2), 61, **2015**.

16. PALMER B.C., PHELAN-DICKENSON S.J., DELOUISE L.A. Multi-walled carbon nanotube oxidation dependent keratinocyte cytotoxicity and skin inflammation[J]. T Particle and Fibre Toxicology, **16** (1), 3, **2019**.

17. LIU Y., ZHANG Y., ZHANG T., JIANG Y., LIU X. Synthesis, characterization and cytotoxicity of phosphorylcholine oligomer grafted graphene oxide[J]. Carbon, **71**, 166, **2014**.

18. WANG D., WANG G., ZHANG G., XU X., YANG F. Using graphene oxide to enhance the activity of anammox bacteria for nitrogen removal[J]. Bioresour Technol, **131**, 527, **2013**.

19. KIM M.J., KO D., KO K., KIM D., JI Y.L., SANG M.W., KIM W., CHUNG H. Effects of silver-graphene oxide nanocomposites on soil microbial communities[J]. Journal of Hazardous Materials, **346**, 93, **2018**.

20. OMID A., ELHAM G. Toxicity of graphene and graphene oxide nanowalls against bacteria[J]. Acs Nano, **4** (10), 5731, **2010**.

21. NGUYEN H.N., RODRIGUES D.F. Chronic toxicity of graphene and graphene oxide in sequencing batch bioreactors: A comparative investigation[J]. J Hazard Mater, **343**, 200-, **2018**.

22. LIU X., ZHAO Y., LUO Y., WANG Y., WANG X. Effect of Graphene Oxide on the Characteristics and Mechanisms of Phosphorus Removal in Aerobic Granular Sludge: Case Report[J]. Water, Air, & Soil Pollution, **229** (1), **2017**.

23. GUO C., WANG Y., LUO Y., CHEN X., LIN Y., LIU X. Effect of graphene oxide on the bioactivities of nitrifying and denitrifying bacteria in aerobic granular sludge[J]. Ecotoxicology & Environmental Safety, **156**, 287, **2018**.

24. AHMED F., RODRIGUES D.F. Investigation of acute effects of graphene oxide on wastewater microbial community: a case study[J]. Journal of Hazardous Materials, **256-257** (1), 33, **2013**.

25. INDRANIL C., DUCH M.C., MANSUKHANI N.D., HERSAM M.C., DERMONT B. Colloidal properties and stability of graphene oxide nanomaterials in the aquatic environment[J]. Environmental Science & Technology, **47** (12), 6288, **2013**.

26. ZENG Q., LI Y., YANG S. Sludge Retention Time as a Suitable Operational Parameter to Remove Both Estrogen and Nutrients in an Anaerobic-Anoxic-Aerobic Activated Sludge System[J]. Environmental Engineering Science, **30** (4), 161, **2013**.

27. SHAN S.J., ZHAO Y., TANG H., CUI F.Y. A Mini-review of Carbonaceous Nanomaterials for Removal of Contaminants from Wastewater[J]. IOP Conference Series: Earth and Environmental Science, **68** (1), 012003, **2017**.

28. China Environmental Science Press, B., China, Water and Waste-water Monitoring and Analysis Methods. National Environmental Protection Agency[J], Editor of water and wastewater monitoring and analysis methods, **1997**.

29. SHENG G.P., YU H.Q., LI X.Y. Extracellular polymeric substances (EPS) of microbial aggregates in biological wastewater treatment systems: a review. Biotechnology Advances, **28** (6), 882, **2010**.

30. WANG R., PENG Y., CHENG Z., REN N. Understanding the role of extracellular polymeric substances in an enhanced biological phosphorus removal granular sludge system[J]. Bioresour Technol, **169** (5), 307, **2014**.

31. CHEN H., ZHENG X., CHEN Y., LI M., LIU K., LI X. Influence of Copper Nanoparticles on the Physical-Chemical Properties of Activated Sludge[J]. Plos One, **9** (3), e92871, **2014**.

32. KOWALCHUK G.A., STEPHEN J.R. BOER W, DE., PROSSER J.I., EMBLEY T.M., WOLDENDORP J.W. Analysis of *ammonia-oxidizing* bacteria of the beta subdivision of the class Proteobacteria in coastal sand dunes by denaturing gradient gel electrophoresis and sequencing of PCR-amplified 16S ribosomal DNA fragments[J]. Appl Environ Microbiol, **63** (4), 1489, **1997**.

33. DIONISI H.M., LAYTON A.C., GERDA H., GREGORY I.R., ROBINSON K.G., SAYLER G.S. Quantification of Nitrosomonas oligotropha-like ammonia-oxidizing bacteria and Nitrospira spp. from full-scale wastewater treatment plants by competitive PCR[J]. Applied & Environmental Microbiology, **68** (1), 245, **2002**.

34. MICHOTEY V., MÉJEAN V., BONIN P. Comparison of methods for quantification of cytochrome cd(1)-denitrifying bacteria in environmental marine samples[J]. Applied & Environmental Microbiology, **66** (4), 1564, **2000**.

35. THROBACK I., K. ENWALL, A., HALLIN S. Reassessing PCR primers targeting nirS, nirK and nosZ genes for community surveys of denitrifying bacteria with DGGE[J]. Fems Microbiology Ecology, **49** (3), 401, **2010**.

36. LI L., KONG X. Experimental study on the treatment of high Cl-high Ca~(2+) and high COD wastewater by activated sludge process[J]. Industrial Water Treatment, **31** (11), 74, **2011**.

37. HAI R., WANG Y., WANG X., DU Z., LI Y. Impacts of Multiwalled Carbon Nanotubes on Nutrient Removal

from Wastewater and Bacterial Community Structure in Activated Sludge[J]. e107345, **2014**.

38. NGUYEN H.N., C.-W.S.L., RODRIGUES D.F., Acute toxicity of graphene nanoplatelets on biological wastewater treatment process[J]. Environ. Sci.: Nano, **4** (1), 160, **2017**.

39. NGUYEN H.N., R.D.F., Chronic toxicity of graphene and graphene oxide in sequencing batch bioreactors: A comparative investigation[J]. Journal of Hazardous Materials, **343**, 200, **2018**.

40. DODDS W.K., SMITH V.H. Nitrogen, phosphorus, and eutrophication in streams[J]. Inland Waters, **6** (2), 155, **2016**.

41. HAI R., WANG Y., WANG X., DU Z., LI Y. Impacts of multiwalled carbon nanotubes on nutrient removal from wastewater and bacterial community structure in activated sludge[J]. Plos One, **9** (9), e107345, **2014**.

42. SHAH R., KAUSAR A., MUHAMMAD B. Characterization and Properties of Poly(methyl methacrylate)/Graphene, Poly(methyl methacrylate)/Graphene Oxide and Poly(methyl methacrylate)/p-Phenylenediamine-Graphene Oxide Nanocomposites[J]. Journal of Macromolecular Science: Part D - Reviews in Polymer Processing, **54** (13), 1334, **2015**.

43. HOU W., MA Z., SUN L., HAN M., LU J., LI Z., MOHAMAD O.A., WEI G. Extracellular polymeric substances from copper-tolerance Sinorhizobium meliloti immobilize Cu^{2+}[J]. Journal of Hazardous Materials, **261** (20), 614, **2013**.

44. BAEK C., C.S.H., KIM J., YOON S., MIN J. Bacterial Adsorption on Nano Graphene Oxide-Coated Microbeads for Molecular Diagnosis[J]. Journal of Nanoscience & Nanotechnology, **16** (11), 11887, **2016**.

45. WANG J., CHEN B. Adsorption and coadsorption of organic pollutants and a heavy metal by graphene oxide and reduced graphene materials. Chemical Engineering Journal, **281**, 379, **2015**.

46. ZHANG X., GONG Y., JIA S., QIN C. Co-adsorption of an anionic dye in the presence of a cationic dye and a heavy metal ion by graphene oxide and photoreduced graphene oxide[J]. RSC Advances, **9** (10), 5313, **2019**.

47. LI X., ZHOU H., WU W., WEI S., XU Y., KUANG Y. Studies of heavy metal ion adsorption on Chitosan/Sulfydryl-functionalized graphene oxide composites[J]. J Colloid Interface Sci, **448**, 389, **2015**.

48. CAROLINE K., CATERINA L., ARJAN B., KARIN T., DICK E., VALTER T., YUNHONG K., JAAP V.D.W., JANNEKE K., SIMONA R. Identity, abundance and ecophysiology of filamentous Chloroflexi species present in activated sludge treatment plants[J]. Fems Microbiology Ecology, **59** (3), 671, **2007**.

SUPPLEMENTARY MATERIAL

Table S1. Removal performances of organic and nutrient in the test SBR.

Items	GO (mg/L)	Test	Control	*P*-value	Items	GO (mg/L)	Test	Control	*P*-value
COD	1	11.61±2.67	5.87±1.13	0.000	TN	1	10.60±4.50	9.61±0.28	0.518
	2	11.21±4.44	5.87±1.13	0.003		2	10.64±3.02	9.47±0.31	0.266
	5	17.09±8.54	5.87±1.13	0.001		5	9.17±2.29	9.52±0.22	0.653
	10	19.22±7.44	6.14±1.29	0.000		10	11.88±3.99	9.45±0.25	0.085
	15	20.56±6.55	6.14±1.29	0.000		15	8.51±1.45	9.59±0.24	0.041
	30	42.52±12.05	5.60±0.84	0.000		30	8.53±0.87	9.41±0.23	0.008
	60	37.40±5.71	6.14±1.29	0.000		60	6.97±2.74	9.33±0.37	0.019
	80	21.89±4.89	6.14±1.29	0.000		80	3.82±1.59	9.10±0.26	0.000
	0	12.02±4.96	6.14±1.29	0.003		0	6.48±2.34	8.92±0.21	0.006
NH_4^+-N	1	3.61±4.89	0.53±0.09	0.075	P	1	0.48±0.81	0.09±0.13	0.164
	2	4.94±3.47	0.42±0.16	0.001		2	0.92±0.79	0.12±0.10	0.007
	5	2.28±2.61	0.53±0.10	0.059		5	1.13±0.77	0.05±0.05	0.000
	10	3.79±3.44	0.42±0.16	0.008		10	1.40±0.78	0.03±0.02	0.000
	15	0.90±1.24	0.53±0.10	0.385		15	0.25±0.25	0.03±0.02	0.018
	30	0.79±0.68	0.42±0.16	0.133		30	0.71±0.60	0.03±0.02	0.003
	60	1.41±1.55	0.30±0.26	0.048		60	1.22±0.51	0.03±0.02	0.000
	80	2.71±1.52	0.01±0.03	0.000		80	0.56±0.31	0.03±0.01	0.000
	0	0.98±0.27	0.01±0.03	0.000		0	0.16±0.15	0.01±0.01	0.009

Table S2. The quality of GO influent and effluent.

GO concentration (mg/L)	Cycle	Influent (mg)	Effluent (mg)	GO concentration (mg/L)	Cycle	Influent (mg)	Effluent (mg)
1	1	2	0	2	1	4	0
	2	2	0		2	4	0
	3	2	0		3	4	0
	4	2	0		4	4	0
	5	2	0		5	4	0
	6	2	0		6	4	0
	7	2	0		7	4	0
	8	2	0		8	4	0
	9	2	0		9	4	0
	10	2	0		10	4	0

Table S2. Continued.

GO concentration (mg/L)	Cycle	Influent (mg)	Effluent (mg)
5	1	10	0
	2	10	0
	3	10	0
	4	10	0
	5	10	1
	6	10	1
	7	10	1
	8	10	0
	9	10	0
	10	10	0
	11	10	0
	12	10	0
	13	10	0
	14	10	0
	15	10	0
	16	10	0
10	1	20	1
	2	20	1
	3	20	1
	4	20	1
	5	20	1
	6	20	1
	7	20	1
	8	20	1
	9	20	1
	10	20	1
15	1	30	1
	2	30	1
	3	30	1
	4	30	1
	5	30	1
	6	30	1
	7	30	1
	8	30	1
	9	30	1
	10	30	1

GO concentration (mg/L)	Cycle	Influent (mg)	Effluent (mg)
30	1	60	1
	2	60	1
	3	60	1
	4	60	1
	5	60	1
	6	60	1
	7	60	1
	8	60	1
	9	60	1
	10	60	1
60	1	120	2
	2	120	2
	3	120	2
	4	120	2
	5	120	2
	6	120	2
	7	120	2
	8	120	2
	9	120	2
	10	120	2
80	1	160	2
	2	160	2
	3	160	2
	4	160	2
	5	160	2
	6	160	2
	7	160	3
	8	160	3
	9	160	3
	10	160	3